

# **HYPERTHERMIA VIA AC ELECTROMAGNETIC FIELD AND MAGNETIC NANOPARTICLES INTEGRATED IN MICRO-CARRIERS NAVIGABLE IN BLOOD VESSELS**

Seyed Nasr Tabatabaei, Sylvain Martel

*Nanorobotics Laboratory, Department of Computer and Software Engineering,  
Institute of Biomedical Engineering, École Polytechnique de Montréal (EPM),  
Montréal (Québec) Canada*

## **INTRODUCTION**

One of the major challenges in finding a suitable therapy for cancer is to save healthy cells while destroying the damaged ones. Hyperthermia is among many suggested methods in which by targeting only cancer cells for treatment, it keeps the healthy cells out of harm. However this approach is still being researched on and far from practical use at the nearby hospital. In this report optimum values for AC magnetic field hyperthermia are theoretically investigated.

Hyperthermia is an abnormal or unusual raise of body temperature. Healthy body cells tolerate excess body heat to a certain level, whereas unhealthy cells such as cancer cells begin to die under these conditions. Healthy cells have organized and systematic networks of veins, blood vessels and neurons that can dissipate heat easily while cancer cells have far less developed neurons and veins [1]. Although high temperatures may become dangerous to both healthy and unhealthy cells, hyperthermia therapy tries to heat body cells to a degree where healthy cells survive and unhealthy cells weaken. Furthermore, cancer cells become more vulnerable to other treatments such as chemotherapy and radiation therapy once they are heated. A temperature range of 42-44 degree Celsius has been determined to be the most adequate for hyperthermia [2].

Hyperthermia can be achieved via one of the three methods: i. Contact with externally heated liquid such as in whole body hyperthermia; ii. Wireless applicators such as high intensity focused ultrasound, microwave, or radio frequency; and iii. Surgical insertion of heating sources (probes, antennas, and capacitive or inductive mediators such as ferromagnetic rods or thermoseeds [3-6]. Although each method has its own advantages and disadvantages compared with another, a common disadvantage to all is the lack of homogenous heat distribution at the target area during the treatment. Cell destruction depends directly on heat and its distribution function. If heat is not uniformly distributed in the tissue, the creation of 'hot spots' in the target area will cause patient's discomfort while the treatment will not be very effective.

Magnetic Nanoparticles (MNP) on the other hand are capable of dissipating uniformly distributed heat at the target tissue once they are placed in an AC magnetic field. This alone is one of the main reasons explaining why they are thought to be a better approach for hyperthermia in oncology. But to allow for target hyperthermia, these MNP will be integrated with therapeutic agent in polymeric micro-carriers of approximately 2 micrometers in diameter and capable of transiting through the smallest capillaries. These micro-carriers will then be navigated towards a target such as a tumor using a method similar to the one described in [7] where a 1.5 mm ferromagnetic bead was navigated in the carotid artery of a living swine. Instead of a large magnetic core, the proposed carriers rely on an agglomeration of magnetic nanoparticles used for propulsion through an induction of magnetic gradients generated by a clinical MRI system, tracking through as local distortion of the magnetic field inside the MRI system, while integrating hyperthermic-based functionality for triggering drug-release and enhancing therapeutic efficacy through as controlled elevation of the temperature that can be monitored using MRI at a specific target location.

The heat generated by MNP via AC magnetic field can be due to three major mechanisms depending on the particle size and their magnetic properties. Large multidomain ferro- or ferrimagnetic materials contain several sub-domains each having their own specific magnetization direction. When these materials are exposed to the AC magnetic field, the sub-domain with magnetization direction along the magnetic field axis elongates and the other ones shrink. This is called "domain wall displacements". Since the magnetization curves for increasing and decreasing magnetic field amplitudes do not coincide, the material demonstrates "hysteresis behavior" and produces heat. In smaller particles such as superparamagnetic nanoparticles, there is no domain wall and therefore hysteresis losses cannot occur. However the external AC magnetic field energy helps magnetic moments to rotate and overcome the energy barrier  $E = KV$  where  $K$  is the anisotropy constant and  $V$  the volume of the magnetic core [8]. This energy is then dissipated when the particle relaxes to its equilibrium orientation. This mechanism is called Néel relaxation. There is also a

third mechanism called Brownian relaxation that causes both multidomain and single domain particles to heat up. In this case energy barrier for reorientation of a particle is given by rotational friction due to the rotation of the entire magnetic particle caused by the AC field torque force on the magnetic moment of the particle. The power of which the magnetic material is heated per gram is given by specific absorption rate (SAR) or specific loss power (SLP).

Heat is generated by an external AC magnetic field of which its frequency and strength are limited by the physiological human body response to high frequency magnetic fields. These responses are stimulation of peripheral and skeletal muscles, possible cardiac stimulation and arrhythmia and non-specific inductive heating of tissue. For biomedical purpose, the frequency has to be higher than 50 kHz to avoid neuromuscular electro-stimulation and lower than 10 MHz for appropriate penetration depth of the RF-field [8]. Studies consider a frequency ( $f$ ) of 80 kHz – 1.2 MHz and a magnetic field strength ( $H$ ) of 0 – 32 kAm<sup>-1</sup>. However the biological safety and tolerable range product of  $H - f$  should be less than 13.4 x 10<sup>8</sup> Am<sup>-1</sup>s<sup>-1</sup> [9]. It is therefore critical to find the right combination of frequency and magnetic field for maximum performance and minimum damage to healthy tissue.

## METHOD AND DISCUSSION

To achieve the highest temperature change in the target tissue, SAR should be at its maximum value and can be estimated as [10]:

$$\text{SAR} = (C_{\text{solvent}} \times m_{\text{fluid}} / m_{\text{particle}}) \times (dT / dt) \quad (1)$$

where  $C_{\text{solvent}}$  is the specific heat capacity of solvent ( $C_{\text{H}_2\text{O}} = 4 \times 18 \text{ J/g/K}$ ),  $m$  is the mass, and  $dT$  and  $dt$  represents the change in temperature over time.

For single domain MNP with a diameter of less than 20 nanometers (nm), SAR is a function of Néel and Brownian relaxation only where SAR due to Néel relaxation is given by [11]:

$$\text{SAR}_{\text{Néel}}(f, H) = \mu_0 \pi \chi''(f) H^2 f / \rho \quad (2)$$

where  $\rho$  is the mass density of the magnetic material, i.e. mass per volume of the MNP. Susceptibility  $\chi''$  is given by

$$\chi''(f) = \chi_0 \phi / (1 + \phi^2) \quad (3)$$

$$\phi = f \tau_{\text{Néel}} \quad (4)$$

$$\tau_{\text{Néel}} = \tau_0 \exp[KV / (kT)], \quad (\tau_0 \sim 10^{-9}) \quad (5)$$

$$\chi_0 = \mu_0 M_s^2 V / (kT) \quad (6)$$

where  $\chi_0$  is the DC susceptibility,  $M_s$  is the saturation magnetization,  $V$  being the mean particle volume with a relaxation time  $\tau_{\text{Néel}}$  depending on the ratio between anisotropy energy  $KV$  ( $K_{\text{Fe}_3\text{O}_4} = 1.35 \times 10^4 \text{ J/m}^3$ ) and thermal energy  $kT$  ( $k = 1.38 \times 10^{-23} \text{ J/K}$ ,  $T = 293 \text{ K}$ ). Hergt *et al.* [11] showed that for superparamagnetic nanoparticles,  $\text{SAR}_{\text{Néel}}$  given above strongly increases with an increase of the particle's size.

Brownian relaxation however depends on the viscous drag in the liquid given by  $12\pi\eta Vf$  where  $\eta$  denotes viscosity ( $\eta_{\text{H}_2\text{O}} = 1 \times 10^{-3} \text{ Pa.s}$ ). This relaxation loss is balanced by the magnetic torque  $T = \mu_0 M_R HV$  where  $M_R$  and  $H$  are the remanent and the field amplitude respectively. SAR taking into account both Brownian and Néel relaxation is given by [12]:

$$\text{SAR} = \pi \mu_0 \chi_0 H^2 f (\omega\tau) / (1 + \omega^2 \tau^2) \quad (7)$$

In Equation (7),  $\tau$  is given by  $1/\tau = 1/\tau_{\text{Brownian}} + 1/\tau_{\text{Néel}}$  where  $1/\tau_{\text{Brownian}}$  is negligible since  $\tau_{\text{Brownian}}$  is 10<sup>3</sup> times larger than  $\tau_{\text{Néel}}$  [13], and  $\omega$  is the angular frequency of the external field. SAR is at its maximum value when  $\omega\tau = 1$ . For  $\tau = \tau_{\text{Néel}}$  maximum SAR could help optimizing frequency and particle's size using Equation (5). And according to M. Ma [10], Brownian power loss is maximum when the particle's diameter ( $d$ ) is

$$d = 2(kT / 8\pi^2 f \eta)^{1/3} \quad (8)$$

Using the above analysis, the frequency vs.  $d$  for maximum SAR due to Néel and Brownian relaxation was plotted in Fig. 1. The straight dotted lines represent upper and lower boundaries for high (10 MHz) and low (50 kHz) biological tissue safety limits [8]. According to Fig. 1, SAR is at its maximum for both Néel and Brownian relaxation at a value  $\omega = 6.28 \times 10^5$  or  $f \approx 100 \text{ kHz}$  ( $Y = 9.672 \text{e}+004$ ). This

value of frequency correspond to an optimum diameter of the MNP of approximately 16 nm ( $X=1.618e-008$ ).

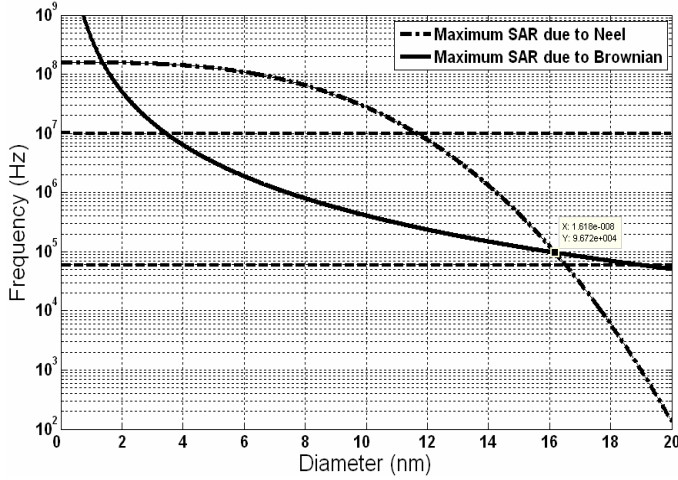


Figure 1: Frequency vs. particle's diameter for maximum SAR due to relaxation.

Néel relaxation becomes negligible for MNP larger than 20 nm [11] while hysteresis losses become more predominant. The larger the hysteresis loop, the greater the SAR. However, Zhang *et al.* [12] showed that due to technical and biocompatibility issues related to medical applications, applied AC magnetic field is much lower than of the saturation field for hysteresis losses of MNP. That is, due to rapid reduced hysteresis loop area with decreasing field amplitude, the loop is far from saturating field. Furthermore, since the full hysteresis loop of such particles cannot be used, single domain MNP with high hysteresis loss become less than suitable for hyperthermia. In addition according to Okawa *et al.* [13], among four MNP samples with concentrations between 4 – 13.5 mg/ml and mean diameters of 7 nm, 18 nm, 40 nm and 80 nm, the target temperature of 43°C was achieved in less than 10 minutes solely when 18 nm MNP were undergone a magnetic field strength ( $H$ ) of 9.5 kAm<sup>-1</sup> (120 Oe) at 120 kHz. This is an empirical proof for the accuracy of the presented graph in Fig. 1. The calculated optimum frequency and particle size are also in close agreement with what is presently being applied *in vivo* for hyperthermia via MNP. Johannsen *et al.* [14] were able to implement a device which uses a variable magnetic field strength of 0 – 18 kAm<sup>-1</sup> at 100 kHz by injecting MNP with  $d = 15$  nm to the tumor. They have successfully performed hyperthermia on various patients.

According to Eq. (2), magnetic field amplitude ( $H$ ) affects the overall SAR value by a factor of 2. However, it is suggested that a high  $H$  field is related to  $\chi_0, \tau_{Néel}$  and frequency as well which leads to a more complex relation between  $H$  and SAR [12]. Nevertheless, since the product of  $H$  and  $f$  should be less than  $13.4 \times 10^8$  Am<sup>-1</sup>s<sup>-1</sup> for safety reasons, substituting 100 kHz for  $f$  will give magnetic field amplitude of 13.4 kAm<sup>-1</sup>. Indeed, numerous experimental studies have shown that field amplitudes of 9 – 11 kAm<sup>-1</sup> are sufficient to cause significant MNP temperature change. In addition, results from Muller *et al.* [15] indicate a magnetic field amplitude of 10 – 15 kAm<sup>-1</sup> as an optimum field amplitude for Fe<sub>3</sub>O<sub>4</sub> MNP of 17 – 21 nm in diameter. In a similar study, Dutz *et al.* [16] show that SAR value for Fe<sub>3</sub>O<sub>4</sub> MNP with 16 nm in diameter is maximum when  $H$  is 10 kAm<sup>-1</sup>.

Equations (3–6) suggest that the physical properties and chemical composition of MNP such as magneto-crystalline anisotropy, magnetization, coating, MNP preparation method and fluid viscosity also affect the loss power and generation of heat. For instance Zhang [12] showed that 19 nm Fe<sub>3</sub>O<sub>4</sub> coated with dextran not only served as a protective shell to minimize direct exposure of the ferrite to the biological environment, but it provided a higher SAR value compared to its uncoated counterpart. In addition, Zhang [12] was able to show that for dextran coated 19 nm Fe<sub>3</sub>O<sub>4</sub> MNP, SAR reaches a maximum when viscosity increases to  $\eta=2 \times 10^3$  Pa.s and decreases thereafter. In other hand, Zeisberger *et al.* [17] confirmed that other metallic nanoparticles such as cobalt in the range of 20 nm in diameter show higher SAR than simple iron oxide particles. This is especially interesting for the purpose of guiding MNP towards the target area. Ferrofluid with cobalt particles has greater magnetization saturation than ferrofluid with iron oxide particles [18], hence potentially increasing by a factor of approximately four the guiding efficiency of ferrofluid cobalt particles to the tumoral lesion where they could be heated as for target hyperthermia.

## CONCLUSION

It was shown that MNP of mean size 16 nm in diameter exert maximum SAR due to both Brownian and Néel if they are placed in a field at 100 kHz frequency. Also, field amplitude of  $\sim 10$  kAm<sup>-1</sup> was

suggested as optimum field amplitude for this purpose. However optimum values for particle size, frequency and field amplitude for maximum SAR may differ theoretically than those of found experimentally. Although it is possible to approximate these values individually, in practice, there are many other unknown and complex factors that affect SAR. Therefore for hyperthermia via AC electromagnetic field and MNP, a first task is to optimize all parameters effecting SAR. To validate these values *in vitro*, an experimental setup is currently under investigation where a 7.5 kW Induction Heating machine (Ameritherm Inc.) connected to 5 turn copper tube coil of 35 mm in diameter will be used. This set up will easily provide the AC field amplitude of  $9 \text{ kAm}^{-1}$  at 150 kHz, corresponding to the theoretical values presented in this paper. Although more experimental results are needed and will be investigated in the future, the results presented in this paper provides valuable data showing the potential of integrating target hyperthermic-based procedures in micro-carriers navigated in the blood vessels towards specific targets for applications such as drug delivery. As such, breaking or melting polymeric shells of these carriers while enhancing therapeutic efficacy can be envisioned.

## REFERENCE

- [1] K. L. Ang, S. Venkatraman, and R. V. Ramanujan, "Magnetic PNIPA hydrogels for hyperthermia applications in cancer therapy," *Materials Science and Engineering C*, vol. 27, pp. 347-351, April 2007.
- [2] W. C. Dewey, L. E. Hopwood, S. A. Sapareto, and L. E. Gerweck, "Cellular responses to combinations of hyperthermia and radiation," *Radiology*, vol. 123, pp. 463-474, May 1, 1977 1977.
- [3] X. Yang, J. Du, and Y. Liu, "Advances in Hyperthermia technology," Shanghai, China, 2005, pp. 6766-6769.
- [4] M. M. Paulides, J. F. Bakker, and G. C. van Rhoon, "Electromagnetic Head-And-Neck Hyperthermia Applicator: Experimental Phantom Verification and FDTD Model," *International Journal of Radiation Oncology Biology Physics*, vol. 68, pp. 612-620, 2007.
- [5] B. S. K. Byeong-Ho Park, Young Kon Kim, Moon Kon Kim, "The Induction of Hyperthermia in Rabbit Liver by means of duplex Stainless Steel Thermoseeds," *Korean Journal of Radiology*, vol. 3, pp. 98-104, 2002.
- [6] T. S. H. Takahashi, H. Motoyama, T. Uzuka, S. Takahashi, K. Morita, K. Kakinuma, R. Tanaka, "Radiofrequency interstitial hyperthermia of malignant brain tumors: development of heating system," *Experimental Oncology*, vol. 22, pp. 186-190, April 20, 2000 2000.
- [7] S. Martel, J.-B. Mathieu, O. Felfoul, A. Chanu, E. Aboussouan, S. Tamaz, P. Pouponneau, L. H. Yahia, G. Beaudoin, G. Soulez, and M. Mankiewicz, "Automatic navigation of an untethered device in the artery of a living animal using a conventional clinical magnetic resonance imaging system," *Applied Physics Letters*, vol. 90, p. 114105, 2007.
- [8] E. Duguet, S. Vasseur, S. Mornet, G. Goglio, A. Demourgues, J. Portier, F. Grasset, P. Veverka, and E. Pollert, "Towards a versatile platform based on magnetic nanoparticles for in vivo applications," *Bulletin of Materials Science*, vol. 29, pp. 581-6, 2006.
- [9] S. Bae, S. W. Lee, Y. Takemura, E. Yamashita, J. Kunisaki, S. Zurn, and C. S. Kim, "Dependence of frequency and magnetic field on self-heating characteristics of NiFe<sub>2</sub>O<sub>4</sub> nanoparticles for hyperthermia," *IEEE Transactions on Magnetics*, vol. 42, pp. 3566-3568, 2006.
- [10] M. Ma, Y. Wu, J. Zhou, Y. Sun, Y. Zhang, and N. Gu, "Size dependence of specific power absorption of Fe<sub>3</sub>O<sub>4</sub> particles in AC magnetic field," *Journal of Magnetism and Magnetic Materials*, vol. 268, pp. 33-39, 2004.
- [11] R. Hergt and S. Dutz, "Magnetic particle hyperthermia--biophysical limitations of a visionary tumour therapy," *Journal of Magnetism and Magnetic Materials*, vol. 311, pp. 187-192, 2007.
- [12] L.-Y. Zhang, H.-C. Gu, and X.-M. Wang, "Magnetite ferrofluid with high specific absorption rate for application in hyperthermia," *Journal of Magnetism and Magnetic Materials*, vol. 311, pp. 228-233, 2007.
- [13] K. Okawa, M. Sekine, M. Maeda, M. Tada, M. Abe, N. Matsushita, K. Nishio, and H. Handa, "Heating ability of magnetite nanobeads with various sizes for magnetic hyperthermia at 120 kHz, a noninvasive frequency," *Journal of Applied Physics*, vol. 99, p. 08H102, 2006.
- [14] M. Johannsen, U. Gneveckow, L. Eckelt, A. Feussner, Wald, Ouml, N. Fner, R. Scholz, S. Deger, P. Wust, S. A. Loening, and A. Jordan, "Clinical hyperthermia of prostate cancer using magnetic nanoparticles: Presentation of a new interstitial technique," *International Journal of Hyperthermia*, vol. 21, pp. 637 - 647, 2005.
- [15] R. Muller, S. Dutz, R. Hergt, C. Schmidt, H. Steinmetz, M. Zeisberger, and W. Gawalek, "Hysteresis losses in iron oxide nanoparticles prepared by glass crystallization or wet chemical precipitation," *Journal of Magnetism and Magnetic Materials*, vol. 310, pp. 2399-2401, 2007.
- [16] S. Dutz, R. Hergt, J. Murbe, R. Muller, M. Zeisberger, W. Andra, J. Topfer, and M. E. Bellemann, "Hysteresis losses of magnetic nanoparticle powders in the single domain size range," *Journal of Magnetism and Magnetic Materials*, vol. 308, pp. 305-312, 2007.
- [17] M. Zeisberger, S. Dutz, R. Muller, R. Hergt, N. Matoussevitch, and H. Bonnemann, "Metallic cobalt nanoparticles for heating applications," *Journal of Magnetism and Magnetic Materials*, vol. 311, pp. 224-227, 2007.
- [18] S. Martel, S. Martel, J. P. Mathieu, F. A. Hinojosa, L. A. Y. L. Yahia, and P. A. P. P. Pouponneau, "Fundamental design rules for the conception of microdevices to be propelled in the blood circulatory system through magnetic gradients generated by a clinical MRI system  
Fundamental design rules for the conception of microdevices to be propelled in the blood circulatory system through magnetic gradients generated by a clinical MRI system," in *Microtechnology in Medicine and Biology, 2005. 3rd IEEE/EMBS Special Topic Conference on*, 2005, pp. 253-256.